JEE Journal of Ecological Engineering

Journal of Ecological Engineering, 2026, 27(7), 206–221
https://doi.org/10.12911/22998993/218700
ISSN 2299–8993, License CC-BY 4.0

Received: 2026.02.20
Accepted: 2026.05.20
Published: 2026.06.01

Sustainable removal of methylene blue from water using a chitosan/date-pit biochar composite: Adsorption behavior and environmental implications

Khattab Sultan Abdullah[1,2], Salwa Hadi Ahmed[2*]

[1] Mechanical Engineering Department, College of Engineering – Al-Sharqat, Tikrit University, Iraq
[2] Environmental Engineering Department, Engineering College, Tikrit University, Iraq
* Corresponding author's e-mail: dr.salwahadi@tu.edu.iq

ABSTRACT

This paper improved the capacity for methylene blue (MB) removal from polluted water by designing a sustainable hybrid adsorbent using chitosan (CS) and date pit biochar (DPB). The hybrid was developed as a solution to the poor performance of raw chitosan within acidic medium, by incorporating it into a porous carbon framework that increases its effective pH model and speed of transfer of mass. It was noted that characterization depicted an increment in the point of zero charge (pHpzc) of 7.0 in the case of the CS/DPB and 6.6 in the case of the raw chitosan, signifying enhanced stability over a wide pH gradient. In adsorption experiments, the hybrid achieved 94–96% MB removal in 40–60 minutes, respectively, which was far better than raw chitosan, which had 20–25% removal at pH 3. Equilibrium data were like the Langmuir model, and the maximum adsorption capacity (q_{max}) was raised by 74% to 30.33 mg/g compared to 17.44mg/g in chitosan. The evolution of kinetics obeyed a pseudo-second-order equation ($R^2 = 0.9997$), where the main process was chemisorption, and it was preceded by hydrogen bonding and π π forces. Its composite also proved its viability as the high performance was maintained in five reuse cycles, which is a promising alternative to sustainable industrial wastewater treatment.

Keywords: methylene blue, chitosan, date-pit biochar, adsorption, isotherm, kinetics, thermodynamics.

INTRODUCTION

The climate instability intensified by rapid population growth and industrial expansion is creating growing pressure on water resources, necessitating the wastewater treatment and reuse as part of the integrated approach to the management of water resources (Fegade et al., 2021). One of the most problematic types of pollutants is dye-laden effluents; out of 100,000 commercial dyes used, many of them are chemically stable, aromatic, and do not readily biodegrade, persist in the aquatic environment, and are linked to long-term environmental and health risks (Ahmed et al., 2024; Rasheed et al., 2026). Methylene blue (MB) is an example of a common cationic dye, and uncontrolled exposure to the dye has been associated with potentially deleterious outcomes (Nodehi et al., 2020). Despite the availability of several treatment technologies, including membrane filtration and advanced oxidation ((Ibrahim et al., 2021; Peramune et al., 2022), adsorption is still one of the most convenient and effective approaches, especially when there are high surface area and an extensive amount of active sites available, i.e. in carbonaceous materials, as well as in agricultural wastes, which are valorized (Ibrahim et al., 2024). Chitosan (CS) is an outperforming bio-based adsorbent because of its -NH2/ -OH functional groups, which allow the binding of pollutants by an electrostatic interaction, hydrogen bonding, and ion exchange, but is frequently improved in its stability and recovery (Ahmed and Abduljabbar, 2023). As such, studies have concentrated on chitosan-based hybrids of carbonaceous/mineral supports to increase stability, surface area, and reusability (Bambal et al., 2025). CS/date pit biochar (CS/DPB) is a good

candidate to enhance MB removal and reusability because, within a circular-economy framework, date pits may be transformed into inexpensive, porous biochar to be used as the input in dye adsorption (Alhemadan et al., 2025). It can be described by the well-established equilibrium and kinetic models concerning its adsorption behavior (Nuruzzaman and Mondal, 2025). Based on this, the present work undertakes the systematic comparison of CS and CS/DP-Biochar under the same operating conditions of the removal of MB by studying the influences of pH, initial dye concentration, dosage of adsorbent, and contact time, and then, the equilibrium and kinetic interpretation were conducted using the Langmuir /Freundlich, PFO/PSO, and Weber-Morris.

MATERIALS AND METHODS

Materials, reagents, and methodology

An experiment in this study used raw chitosan (CS) as the main adsorbent for the removal of methylene blue (MB) from aqueous solutions. Also, date-pit biochar (DPB) was made and mixed with chitosan to make a hybrid composite adsorbent (CS/DPB) in mass ratios of 40% biochar: 60% chitosan (w/w) according to literature-reported procedures of making date-pit biochar (Loryuenyong et al., 2024). Methylene blue ($C1_6H_{18}N_3ClS$); molecular weight: 319.85 g/mol) was used as the test contaminant and measured by UV-Vis spectrophotometry at 664nm (Goksu and Tanaydin, 2017). Adsorption experiments were done with initial concentrations of 5–40 mg/L of the MB solutions and adsorbent doses of 0.1–0.5 g to 100 mL of MB solution (initial concentration: 20 mg/L) in 250 mL conical flasks by shaking at 150 rpm and 25 ± 2 C (laboratory temperature) to determine adsorption behavior. Solution pH was measured by using HCl and NaOH. In some instances, methanol (CH_3OH) was used optionally to eliminate traces of organic dye during chitosan preparation (Hosney et al., 2025). Distilled water was used to prepare all the solutions. All aqueous solutions were prepared in the laboratory using distilled/deionized water. All experiments were conducted in duplicate/triplicate, depending on the experimental design, and the results were reported as mean values; in the case of triplicate measurements, the results were expressed as mean ± standard deviation (SD).

Dye adsorption mechanisms by chitosan

Chitosan adsorbs dyes through several mechanisms, mainly:

- Electrostatic attraction: At low pH, $–NH_2$ groups are protonated to $–NH_3^+$, leading to strong attraction toward negatively charged dyes (especially $–SO_3^-$ groups).
- Ion exchange: Exchange of counter-ions with protons associated with $–NH_3^+$ sites; this often occurs simultaneously with electrostatic attraction.
- Hydrogen bonding: Hydrogen bonds can form between –OH and –NH groups in chitosan and functional groups on dye molecules, helping stabilize adsorption.
- π–π interactions: These are more pronounced in chitosan composites containing carbonaceous materials/graphene oxide, particularly with aromatic dyes.
- Complexation/coordination (chelation): Dyes containing metals may bind via chitosan's amino and hydroxyl groups.
- Van Der Waals/hydrophobic interactions: Auxiliary forces that enhance adsorption, especially in less polar systems and composite materials (Manubolu et al., 2024; Patel and Uppaluri, 2025; Shehab et al., 2025), as shown in Figure 1.

The capacity of adsorption (q) in mg/g was determined using Equation 1 (Song et al., 2024):

$$q = \frac{(C_\circ - Cf)}{m} \cdot V \quad (1)$$

where: C_o and Cf – the initial and final concentrations of dye solution in mgL^{-1}, m – the mass of CS and CS/DPB adsorbent in g, V – the volume of dye solution in L.

Removal effectiveness (R%) of each dye was calculated using Equation 2 (Shehab et al., 2025):

$$R\% \frac{(c_\circ - cf)}{c_\circ} \cdot 100 \quad (2)$$

Preparation of adsorbents

Preparation of raw chitosan (CS)

To convert the shell of shrimp into chitosan, successive chemical steps were performed: demineralization at the conditions of 1% (v/v) HCl in the presence of a stirring/heating mixture and subsequent washing to close to the normal pH level (Gamal et al., 2025), deproteinization at a constant temperature and contact time using

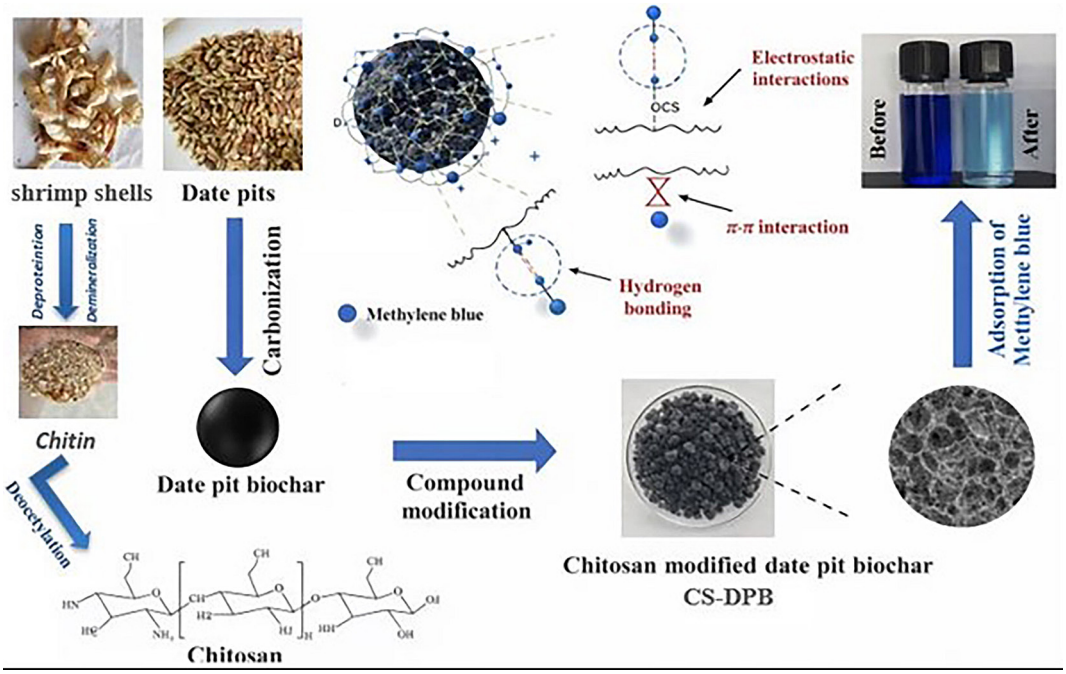

Figure 1. Schematic illustration of the adsorption mechanism/mode of methylene blue (MB) (a cationic dye) onto a chitosan/date pit biochar composite for methylene blue removal from water

NaOH (1–3.5 M), and subsequently deacetylation with NaOH (30–50% w/w) followed by washing to neutral pH. In case of necessity, final drying was done by optional use of methanol to eliminate residual organic dyes (Hosney et al., 2025).

Preparation of date-pit biochar (DP-BC)

Date pits were gathered, thoroughly washed, and allowed to dry in the sun for seven days. The ground and sieved material were dried pits that were sieved using a 100-um mesh to get homogeneous grain-size particles. Pyrolysis was carried out on nitrogen purged muffle furnace in an oxygen-limited/oxygen-free environment. The temperature was set on 650 °C (1h) and left to run in the furnace; the resulting biochar was then left to cool in the furnace to room temperature (Mahdi et al., 2015).

Preparation of the composite adsorbent (CS/DBC)

The hybrid composite adsorbent CS/DBC was made by mixing the date-pit biochar with the raw chitosan in the proportion of 40:60 (w/w) (Loryuenyong et al., 2024), to form an adsorbent that would actually incorporate the functional groups of chitosan and the pore network structure of biochar (Mahdi et al., 2015). A 40:60 ratio (biochar: chitosan) was chosen as the 'optimal synergistic point' based on preliminary experiments balancing adsorption efficiency and structural stability; this ratio ensures the provision of effective functional groups without causing brittleness of the compound (when biochar is increased) or pore closure (when chitosan is increased).

Characterization of the composite (CS/DBC)

The scanning electron microscopy (SEM) method was used to characterize the surface morphology of the CS/DBC composite, the Fourier transform infrared (FTIR) method was used to identify functional groups, the X-ray diffraction (XRD) method to measure the crystalline/amorphous characteristics, and the BET method to measure the specific surface area and pore characteristics of the CS/DBC composite.

Preparation of methylene blue solutions and calibration curve

A stock MB solution with a concentration of 500 mg/L was made by dissolving 0.5 g of MB dye in 1L of distilled water. Different concentrations of the working solutions were diluted accordingly. An absorbance of the MB standards with known concentrations at 664 nm was measured using a UV-Vis spectrophotometer, and a standard curve was developed between the absorbance and the concentration (Vigneshwari and Gokula, 2018).

Batch adsorption experiments for methylene blue removal

To evaluate the effect of pH at (3–7) by adjusting the pH with 0.1 M HCl or 0.1 M NaOH and the contact time by the effect of 20 to 160 min, batch adsorption experiments were done to remove methylene blue (MB) with either pH using CS or CS/DBC composite and a constant agitation speed of 1 50 rpm. Bases of adsorbent dose fluctuated between 0.1–0.5 g/100 mL, and the initial concentration of MB was put at 5–40 mg/l. Following the adsorption step, the samples were centrifuged at 3000 rpm for 15 min, followed by the determination of the remaining concentration of MB through the use of UVv is at 664 nm (Goksu and Tanaydin, 2017). At a constant value of the other factors, temperatures of 25, 35, and 50 °C were examined.

Calculations (removal efficiency and adsorption capacity)

The equilibrium adsorption capacity (q_e, mg/g) and removal efficiency (%) were calculated using standard mass-balance equations based on initial and final dye concentrations, solution volume, and adsorbent mass (Huang et al., 2014).

RESULTS AND DISCUSSION

Characterization of adsorbents

X-ray diffraction (XRD)

XRD results of the CS/DPB composite at the pre-adsorption and post-adsorption of methylene blue (MB) confirmed that there was a semi-crystalline chitosan phase overlaid over the disordered carbon structure of biochar, with a primary peak at 2θ – approximately 20° and weaker peaks in the 28–32° range (Sun et al., 2023). The broadening of the peak and the background is high, which means that the amorphous fraction is high, which is generally caused by a large number of active sites of the surface, which are favorable to adsorption (Chieng et al., 2017). (Chieng et al., 2017). Following MB uptake, a few changes were detected (minor loss of peak intensity and minimal significant enlargement), but no new crystalline phases appeared, indicating that adsorption takes place on or close to the surface with contraction of chitosan chains or any biochar structure in barely significant amounts (Zhou et al., 2023). These partial differences facilitate reactions between MB and -OH/-NH_2 groups and do not change the overall composite structure (Gao et al., 2022), as shown in Figure 2.

FTIR spectroscopy

The FTIR spectra of the CS/DPB composite, post the adsorption of MB (Figure 3), elucidate the functional groups (surface) that participated in the adsorption of the dye. A broad, strong band at 3435 cm^{-1} before the adsorption denotes overlapping O-H and primary amine (-NH_2) vibrations, and 2920 and 2850 cm^{-1} indicate aliphatic CH stretching. The C=O stretching and the NH bending of the polysaccharide backbone are linked to the 1630-1640 cm^{-1} (amide I) region and the band at around 1560 cm^{-1} (amide II). The 1150–1020 cm^{-1} range is attributed to C-O-C/C-O vibrations of glycosidic bonds and oxygenated surface groups on the biochar, active adsorption sites.

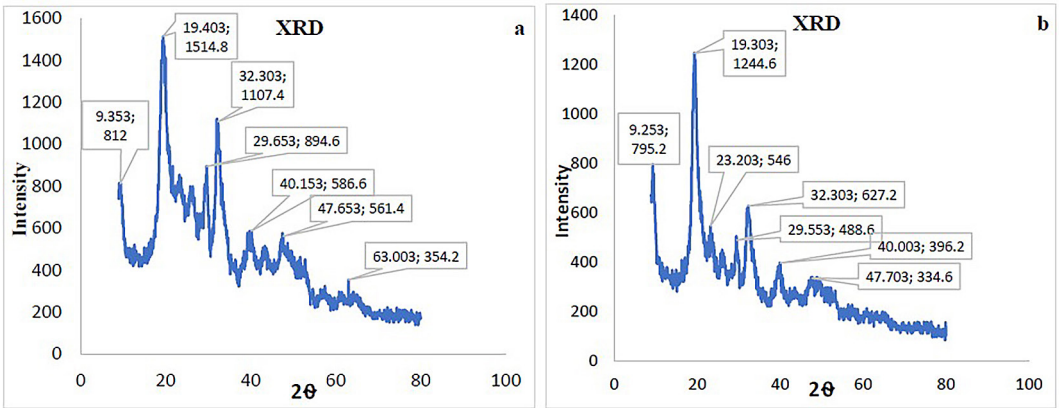

Figure 2. XRD patterns of: (a) the CS/DPB composite before adsorption, and (b) the CS/DPB composite after adsorption of methylene blue

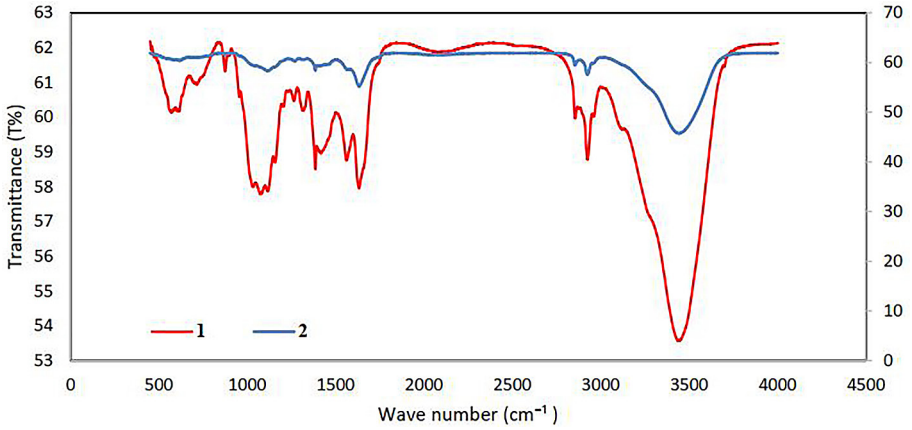

Figure 3. FTIR spectra of: (1) the CS/DPB composite (date-pit biochar blended with chitosan), and (2) the CS/DPB composite after loading with MB dye

The fact that after MB uptake, the intensity of the band at 3435 cm^{-1} has significantly dropped, and the intensity of the bands at 1630 and 1560 cm^{-1} has shifted slightly, denotes that -OH/-NH_2 and C-O functionalities undergo hydrogen bonding and electrostatic interactions with the cationic dye. These data conform to the reported MB adsorption on chitosan-carbon composites (Badran and Khalaf, 2020).

Surface morphology by FESEM

FESEM was used to investigate the morphology of the CS/DPB composite surface and correlate it with the performance on adsorption (Roy et al., 2022). The surface of the pristine composite (Figure 4a) is rough, heterogeneous, comprising grooves, cracks, open pores, irregular carbonaceous particles, showing it has a high accessible surface area and can have active sites that prefer MB adsorption. Once MB is up taken (Figure 4b), the surface gets smaller and some pores/openings are covered partially or completely by granular deposits, which can be explained by the fact that MB is fixed on active sites through electrostatic interactions, hydrogen bonding, andπ3polar interactions with the aromatic porous-carbon structure, similar to what was observed with cationic dye adsorbed by chitosan/biochar systems (Ma et al., 2024)

BET analysis

Nitrogen physisorption As a method of calculating the specific surface area and pore volume, which are fundamental determinants of interpreting dye adsorption in contaminated water, the

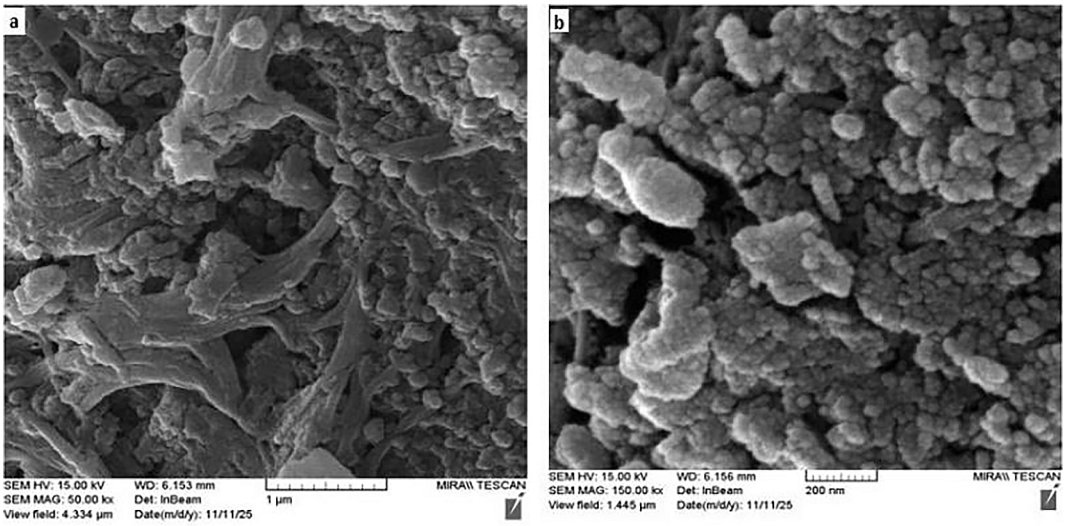

Figure 4. Field-emission scanning electron microscopy (FESEM) images of the chitosan/date-pit biochar composite (CS/DPB): (a) before dye adsorption, (b) after adsorption of methylene blue dye

BET method, relying on the principle of nitrogen physisorption, is one of the most commonly used (Osterrieth et al., 2022). In this research, the BET surface area of the chitosan/date-pit biochar composite 563.75 cm^2/mg was 563.75 cm^2 /mg of the dry weight before adsorption and 431.91 cm^2/mg after the uptake of methylene blue. Similarly, the total pore volume decreased to 0.1217 and 0.1017 cm^3 /g, and the average pore diameter still stayed within the mesoporous range (8.6–9.4 nm). Such decreases in the amount of surface area and the volume of the pores are due to the presence of the dye molecules, which occupy the active pores, partially preventing them from being utilized by the surface, and this implies that it is a successful adsorption and not structural degradation. Mesoporous structure retention is still beneficial to water-treatment applications since mass transfer and intraparticle diffusion are favored, and thus the limitation of internal diffusion is minimized. Moreover, biochar carbon domains must help through the contribution of the π -π interaction with the MB aromatic ring, and chitosan polar functional groups also achieved extra binding through the electrostatic and hydrogen-bonding interactions (Yao et al., 2020), as shown in Figure 5.

PH_{PZC} test

One parameter that is relevant to the interpretation of adsorption is the point of zero charge (pHpzc): the pH at which the adsorbent surface bears an approximately zero net charge. It is usually established through the pH-drift technique, according to which pH is considered to be pHpzc (Neusatz Guilhen et al., 2022). In the study, the MB solutions were determined to be pH 3.0, 4.0, 6.5, 7.0, 9.0, and 10 with the help of 0.1 M HCl/NaOH. The pHpzc of CS and CS/DPB were 6.60 and 7.0, respectively; hence, at pH below the pHpzc, the surface is positively charged, and as the pH approaches or passes pHpzc, the surface turns progressively negatively charged, and it is crucial in absorbing the cationic dye MB+ (Dastoom, 2023). CS low removal (pH 3.0) in the presence of amines due to protonation, electrostatic repulsions with MB +, and H + competition with active sites, and high removal near neutrality (75–82) decreased with protonation (Neusatz Guilhen et al., 2022). By contrast, CS/DPB started with high and changed insignificantly removal (94–96) and reached equilibrium earlier (4060 min) within the entire range of tested pH, which is explained by the biochar porous structure and other adsorption sites/pathways, which cause it to be less sensitive to pH (Hevira et al., 2024), as shown in Figure 6.

EFFECT OF OPERATING PARAMETERS ON METHYLENE BLUE REMOVAL

Effect of PH

The adsorbent surface charge and ionization of functional groups, which is directly regulated by solution pH, determine the efficiency of MB adsorption. At neutral pH, chitosan rather easily removed the biofilm (removal was 75–82 percent at pH 7 compared to about 20–25 percent at pH 3) because the amines were protonated (–NH_2 -NH_3+) and repelled each other electrostatically

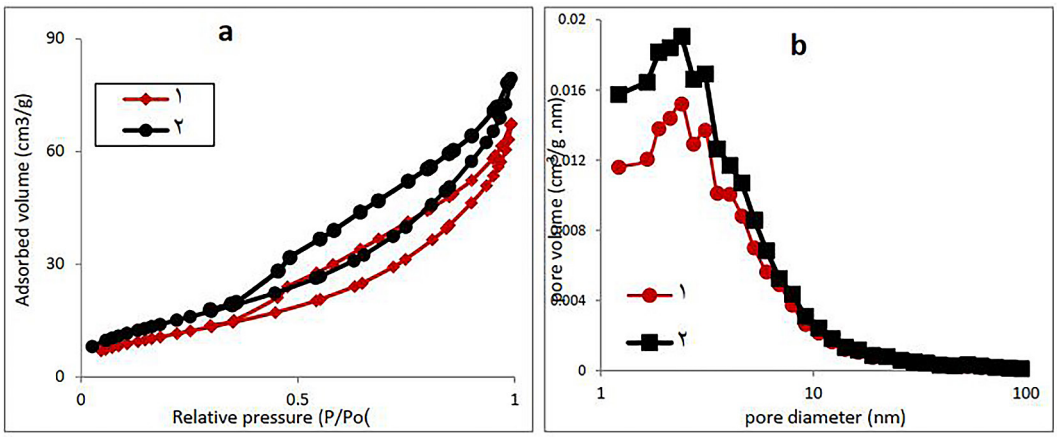

Figure 5. (a) BET nitrogen adsorption–desorption isotherms and (b) pore size distribution curves of the chitosan/date-pit biochar composite, where (1) represents CS/DPB (MB) after MB loading/adsorption treatment, (2) represents CS/DPB (chitosan blended with date-pit biochar) before methylene blue adsorption

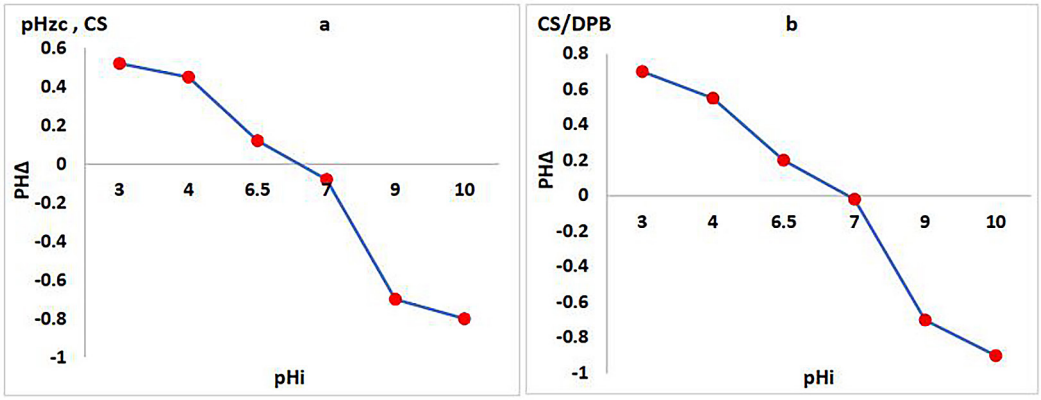

Figure 6. The point of zero charge (pHpzc) tests for (a) raw chitosan (CS) and (b) the chitosan/date-pit biochar composite (CS/DPB)

as well as competed with the active sites, whereas in the case of the raw chitosan, removal was inhibited (poor removal of the biofilm was observed at pH 3, about 20–25 percent). Conversely, higher and faster removal (approximately 94–96 percent in 40–60 minutes). This stability is attributed to raising the compound's zero charge point (pHpzc = 7.0) and the multiplicity of surface bonding forces. While chitosan is critically dependent on electrostatic attraction, the incorporation of biochar provided additional charge-insensitive mechanisms such as π–π stacking interactions between aromatic rings and dye molecules, hydrogen bonds, and the structural role of micropores in physical retention. This synergy between chitosan and biochar gave the compound a "shielding" effect, reducing the sensitivity of the adsorption process to pH changes, thus explaining its operational superiority over crude chitosan (Abd El-Monaem et al., 2024; Liu et al., 2022; Abd El-Monaem et al., 2024), as shown in Figure 7.

Effect of initial concentration

The initial concentration of dye influences adsorption through a driving force of mass-transfer and the time of the method to achieve equilibrium at a constant dose and temperature. The removal of the MB by the raw chitosan (40 mg/L) leads to higher contact time and concentration reaching a peak at about 2030 mg/L (as shown in Figure 8a,b) as the time increases and optimal concentration gradient, however, at maximum concentration (40 mg/L), the MB removal tends to remain Equilibrium yet may increase at adsorption capacity (q_e) (Kellner-Rogers et al., 2019). Conversely, the CS/DPB composite continued to have highly high removal (~95–97%) at the major part of the concentration range and a faster equilibrium, which is a product of the contribution of biochar in terms of higher surface area/porosity and additional aromatic/oxygenated sites in a synergistic relationship with chitosan amino groups (Sharma et al., 2024).

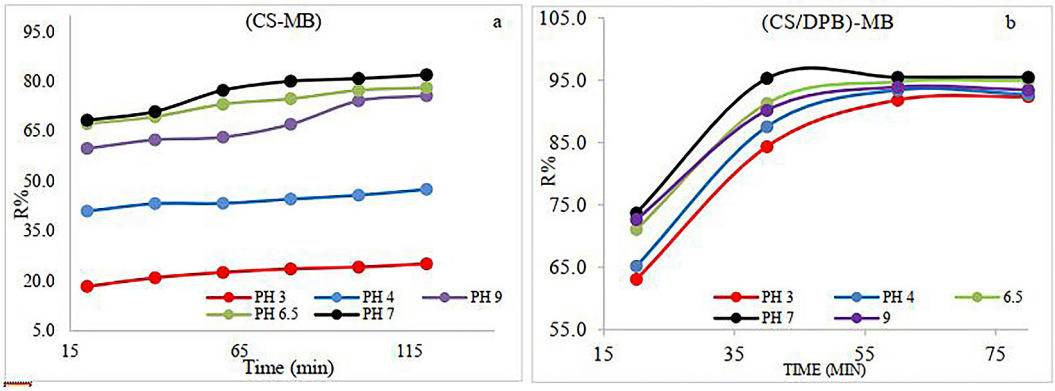

Figure 7. Effect of pH and contact time on the removal efficiency of methylene blue at an initial dye concentration of 20 mg/L, an adsorbent dose of 0.1 g/100 mL, and a temperature of 25 °C, using two adsorption systems: (a) MB removal using raw chitosan, (b) MB removal using the composite (CS/DPB)

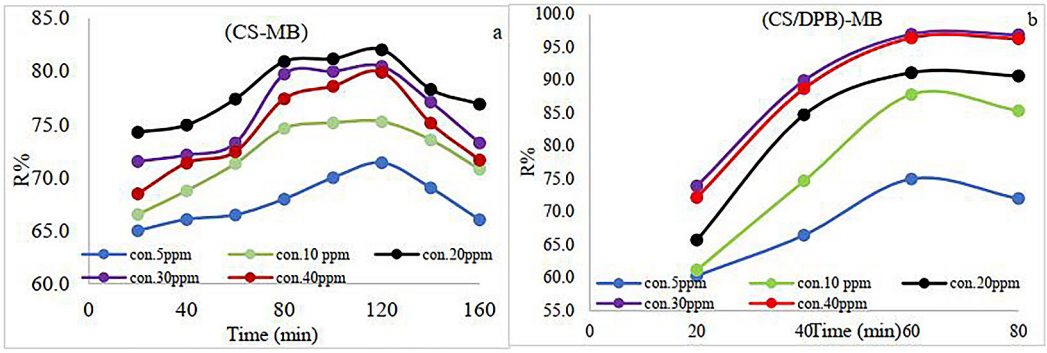

Figure 8. Effect of the initial methylene blue concentration and contact time on the removal efficiency at initial dye concentrations of 5–40 mg/L, an adsorbent dose of 0.1 g/100 mL, and a temperature of 25 °C, with the pH fixed for each adsorption system as follows: (a) MB removal using raw chitosan at pH =7, (b) MB removal using the chitosan/date-pit biochar composite (CS/DPB) at pH = 7

Effect of adsorbent dosage

An "optimal dosage" behavior was observed for MB removal. In the MB/CS system (Figure 9a), the maximum removal (~82% at ~120 min) occurred at 0.1 g, followed by a decline at higher dosages (approximately ~69% at 0.2 g, ~46% at 0.3 g, ~38% at 0.4 g, and ~29% at 0.5 g). This decline can be attributed to particle aggregation and site masking, as well as a reduced effective concentration driving force and increased diffusion resistance within aggregated particles (Rápó and Tonk, 2021). In the MB/CS–DPB system (Figure 9b), the composite maintained very high and near-constant removal within 40–60 min (~97.6–97.7% at 0.1–0.2 g), with only slight decreases at higher dosages (0.3–0.5 g). This reflects abundant and well-distributed active sites and reduced chitosan-chain aggregation due to the presence of a mesoporous carbon surface, which provides faster diffusion pathways and additional π–π interaction sites (Ebrahimzadeh and Akbari, 2025).

Temperature optimization

The range of temperatures (25, 35, 50 °C) was subjected to 20–100 min. At 25 °C (approximately 81 percent at approximately 80 minutes), the highest degree of removal was observed and reduced between 35 and 50 °C, which indicated exothermic adsorption at the MB/CS system (Farasati Far et al., 2024). CS/DPB, in contrast, displayed synergistic, increased uptake with approximately 96.4–97.8% at 25 °C, taking approximately 60 min; removal was almost constant with 0.102 g 97.6–97.7% removal at low concentrations with only slight deviations with increased

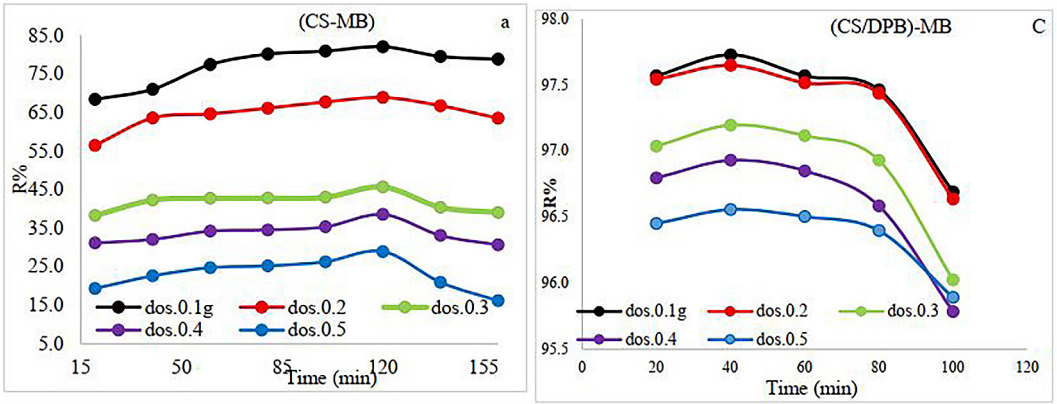

Figure 9. Effect of adsorbent dose and contact time on MB removal efficiency at doses of 0.1–0.4 g/100 mL and a temperature of 25 °C, with the initial dye concentration and pH fixed for each adsorption system as follows: (a) MB removal using raw chitosan at C_0 = 20 mg/L and pH ≈ 7; (b) MB removal using the chitosan/date-pit biochar composite (CS/DPB) at C_0 = 30 mg/L and pH 7

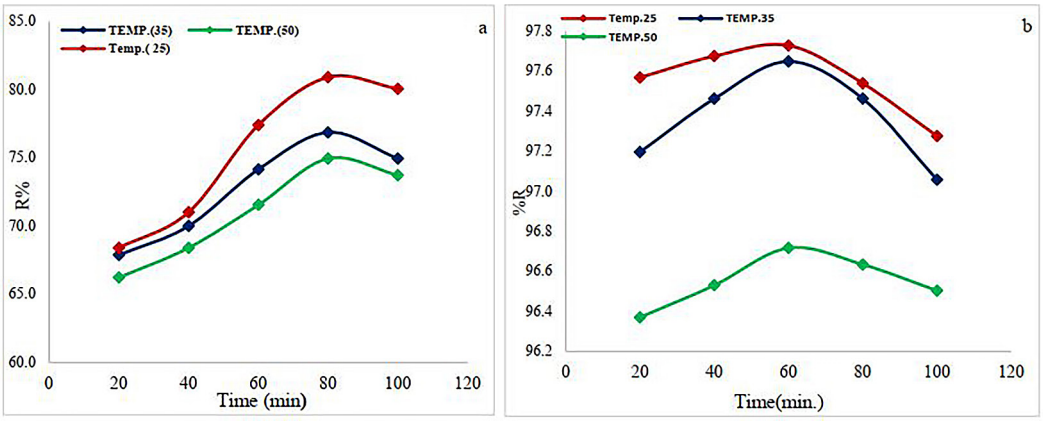

Figure 10. Effect of solution temperature and contact time on MB removal efficiency at 25, 35, and 50 °C and contact times of 20, 40, 60, 80, and 100 min, under fixed operating conditions (constant adsorbent dose, constant agitation, and controlled pH), with the initial dye concentration (C_0) fixed for each adsorption system as follows: (a) MB removal using raw chitosan (CS) at C_0 = 20 mg/L and pH =7; and (b) MB removal using the chitosan/date-pit biochar composite (CS/DPB) at C_0 = 40 mg/L and pH = 7

dosage, indicating that there is limited aggregation and increased diffusion in the mesoporous structure. (Ebrahimzadeh and Akbari, 2025), as shown in Figure 10.

ADSORPTION ISOTHERM

Equilibrium analysis of the methylene blue adsorption in both raw chitosan and the CS/DPB

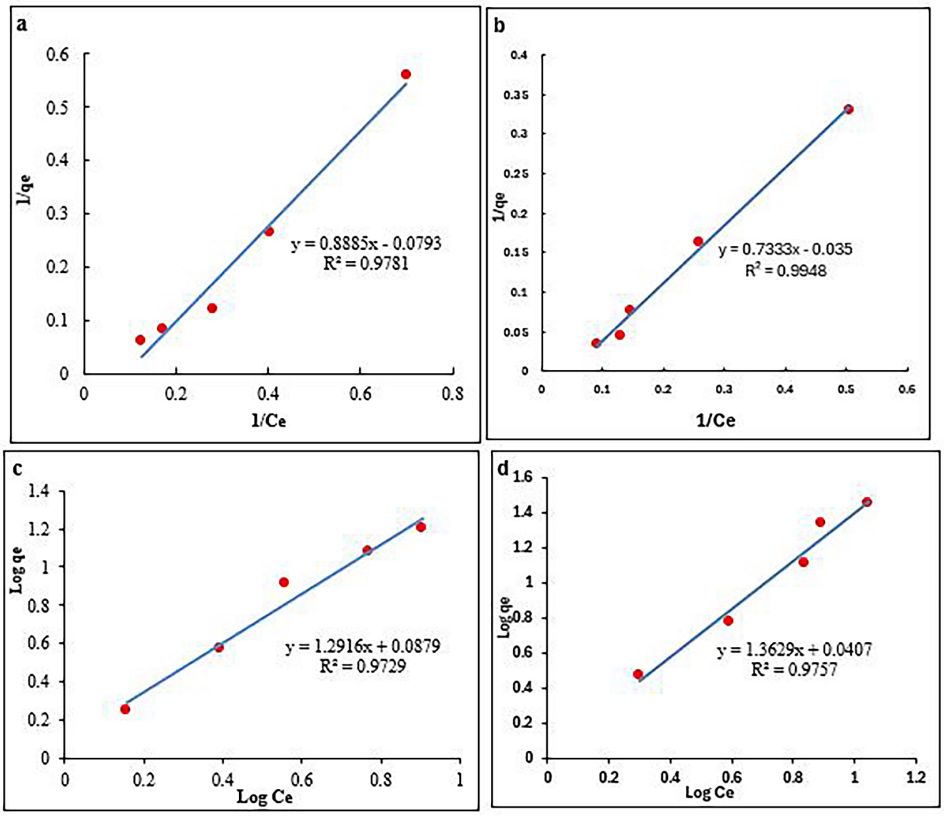

Figure 11. Linearized isotherm plots and the corresponding fitting curves for methylene blue (MB) adsorption onto raw chitosan (CS) and the chitosan/date-pit biochar composite (CS/DPB): (a) Langmuir isotherm for MB adsorption onto CS; (b) Langmuir isotherm for MB adsorption onto CS/DPB; (c) Freundlich isotherm for MB adsorption onto CS; (d) Freundlich isotherm for MB adsorption onto CS/DPB

Table 1. Langmuir and Freundlich adsorption isotherm parameters for the removal of methylene blue using raw chitosan and the chitosan/date-pit biochar composite (CS/DPB)

Langmuir model				Freundlich model			
Adsorbent	q_m (mg/g)	K_c(L/mg)	RL	R^2	1/n	K_f(mg/g)	R^2
CS	17.44	0.271	0.145	0.9781	0.774	7.575	0.9729
CS/DPB	30.33	0.458	0.229	0.9948	0.733	0.54907	0.9757

adsorbent shows that the Langmuir model is more appropriate to describe the data of the adsorption process than the Freundlich. In the case of CS, Langmuir demonstrates a little better goodness of fit (R^2 = 0.9781) in comparison with Freundlich (R^2 = 0.9729), but it supports a monolayer adsorption on rather homogeneous active sites dominated by chitosan -NH_2/ OH^- groups, predominantly (Ge et al., 2022). Similarly, CS/DPB has an excellent performance of Langmuir behavior (R^2 = 0.9948 vs. 0.9757) with a superior maximum capacity value (q_{max} = 30.33 mg/g vs. 17.44 mg/g between CS and MB) and excellent Langmuir affinity of constant (Kc = 0.458 vs. 0.271847 L/mg), meaning enhanced apparent affinity and uptake by MB. As shown in Figure11 and Table 1, the Langmuir and Freundlich parameters and the values of R^2 (Al-Ghouti and Da'ana, 2020).

KINETIC STUDY

Pseudo-first order (PFO) and pseudo-second order (PSO) kinetic models were juxtaposed regarding plot linearity, R^2, and qn. The PSO model was the best fit for the two systems (CS: R^2 = 0.99; CS/DPB: R^2= 0.99756) compared to the PFO model. It means that the adsorption rate is primarily determined by active-site coverage and the

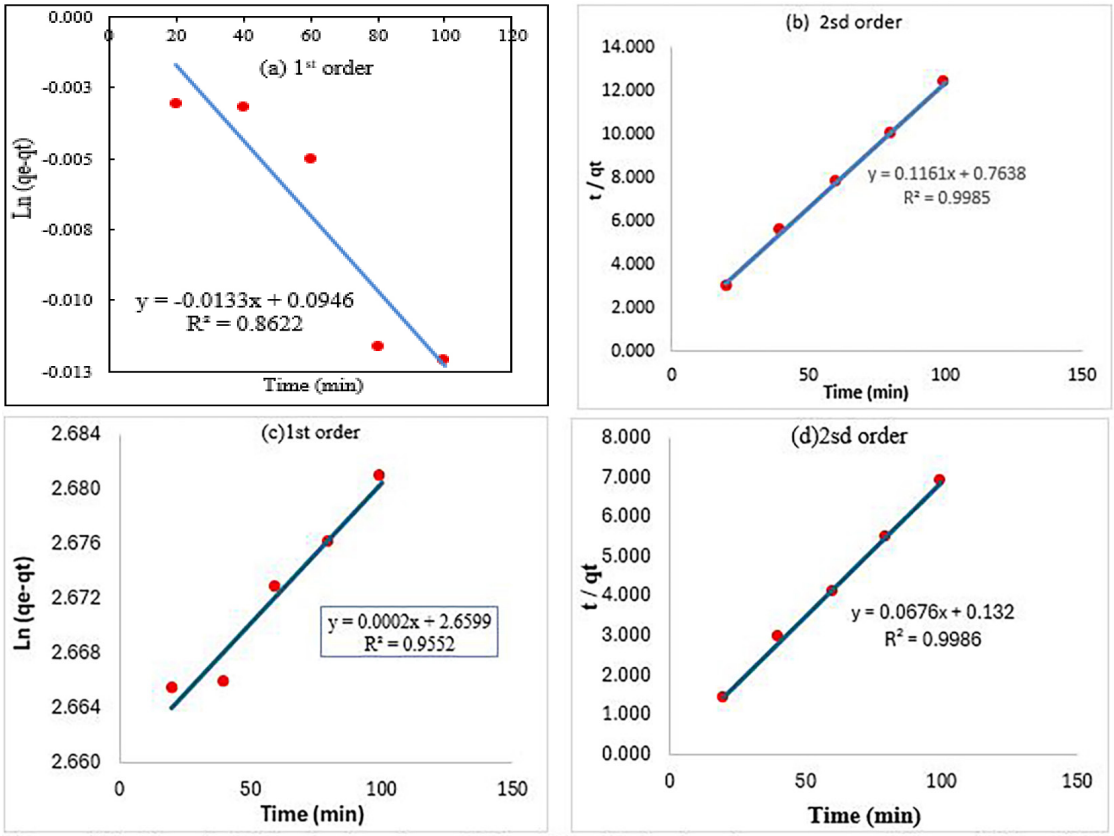

Figure 12. Linearized kinetic plots for methylene blue adsorption onto raw chitosan and the chitosan/date-pit biochar composite (CS/DPB) using the pseudo-first-order and pseudo-second-order models: (a) pseudo-first-order plot for MB adsorption onto CS; (b) pseudo-second-order plot for MB adsorption onto CS; (c) pseudo-first-order plot for MB adsorption onto CS/DPB; (d) pseudo-second-order plot for MB adsorption onto CS/DPB

equilibrium method, which is mentioned in most cases of the chitosan and carbonaceous porous sorbents (Parlayıcı and Baran, 2025). As shown in Figure 12 and Table 2, the kinetic constants, q_e, and the value of R^2. To discuss the mass transfer contributions. The Weber-Morris intraparticle diffusion model was also used. As shown in Figure 12 and Table 3, the plots revealed that intraparticle diffusion is not the only rate-limiting step, as they were well linearized ($R^2 = 0.9552$ with a positive intercept), indicating that boundary-layer (film) diffusion also played a role in MB uptake.

DESORPTION THERMODYNAMICS

Van't Hoff curve of Figure 14 and the thermodynamic quantities in Table 4. The thermodynamic parameters (ΔG°, ΔH°, and ΔS°) were evaluated using the Van't Hoff equation based on the temperature-dependent equilibrium constant (KL). For both CS and CS/DPB systems, the negative values of ΔG° at 298 K (−4.13 and −9.89 kJ/mol, respectively) confirm that methylene blue adsorption is thermodynamically favorable and spontaneous (Aljeboree et al., 2017). The negative ΔH° values (−3.36 kJ/mol for CS and −12.55 kJ/mol for CS/DPB) indicate that the adsorption process is exothermic in nature, suggesting that the interaction between MB molecules and active sites on the adsorbents is energetically favorable (Sulyman et al., 2018). Moreover, the negative ΔS° values (−136.9 and −10.44 J/mol·K, respectively) imply a decrease in randomness at the solid–solution interface during adsorption, which is attributed to the immobilization of dye molecules onto the adsorbent surface (Aljeboree et al., 2017). Overall, the thermodynamic results demonstrate that MB adsorption onto CS and CS/DPB is feasible, spontaneous, and exothermic, with CS/DPB exhibiting a more favorable energetic profile as evidenced by its more negative ΔG° and ΔH° values (Abbas et al., 2021; Okorocha et al., 2021).

COMPARISON WITH PREVIOUS STUDIES ON MB REMOVAL

To benchmark the performance of the present work, recent literature on MB adsorption using low-cost and sustainable adsorbents was surveyed. As shown in Table 5, the adsorption capacity of the CS/DPB composite (30.3 mg/g)

Table 2. Kinetic parameters of pseudo-first order (PFO) and pseudo-second order (PSO) models for methylene blue adsorption onto raw chitosan and the chitosan/date-pit biochar composite (CS/DPB)

	Pseudo-first-order kinetic model			Pseudo-second order kinetic model		
Adsorbent	q_e(mg/g)	K_1	R^2	q_e(mg/g)	K_2	R^2
CS	3.303	-0.000569	0.9716	8.613	0.018	0.9985
CS/DPB	10.155	0.000746667	0.8855	13.550	-0.017	0.9986

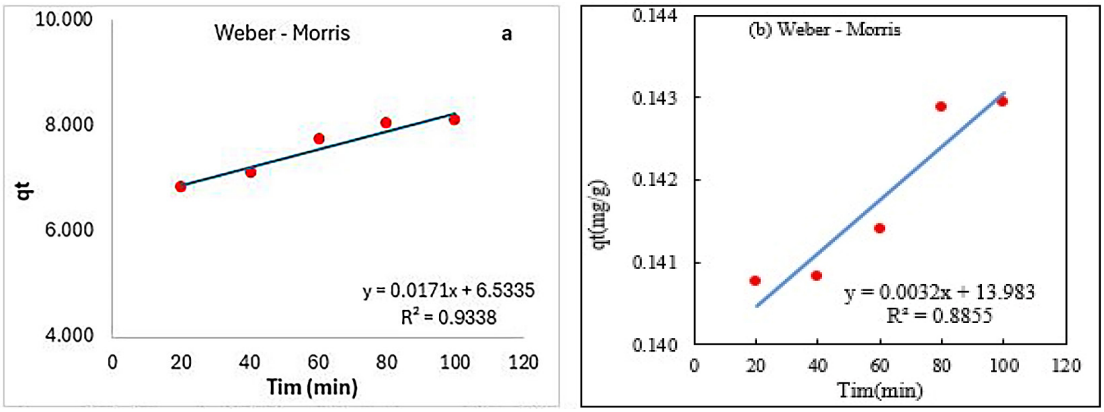

Figure 13. Linearized Weber–Morris intraparticle diffusion plots for methylene blue adsorption onto raw chitosan and the chitosan/date-pit biochar composite (CS/DPB): (a) Weber–Morris plot for MB adsorption onto CS; (b) Weber–Morris plot for MB adsorption onto CS/DPB

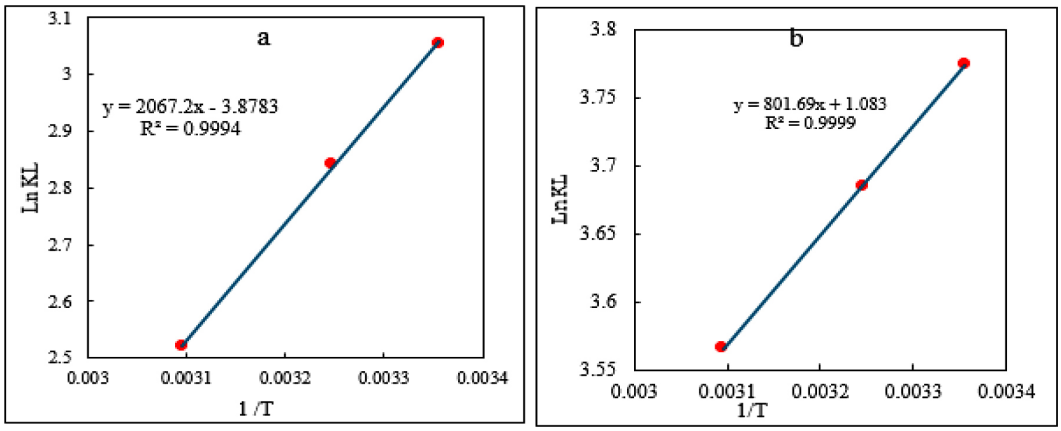

Figure 14. Van't Hoff thermodynamic plots (ln K_L) versus (1/T) for methylene blue adsorption: (a) MB adsorption onto raw chitosan; (b) MB adsorption onto the chitosan/date-pit biochar composite (CS/DPB)

Table 3. Weber–Morris intraparticle diffusion model parameters (k_{id} and C) for methylene blue adsorption onto raw chitosan and the chitosan/date-pit biochar composite (CS/DPB)

Weber–Morris			
Adsorbent	Slope	Kid	R^2
CS	0.0838	0.002	0.9338
CS/DPB	0.07018	0.00107	0.9552

is higher than that of many reported low-cost chitosan-based and biochar-based adsorbents. This confirms that incorporating date-pit biochar into the chitosan matrix significantly enhances adsorption performance while maintaining sustainable and low-cost characteristics.

DESORPTION AND REUSABILITY

The reusability characteristics of MB removal were analyzed with AR cycles of EDTA-regeneration between CS and CS/date-pit biochar (Figure 15). Five cycles later, the adsorption capacity of CS reduced to 16.408 and 9.518 mg/g, whereas the supported composite had higher values of 29.028 and 22.702 mg/g and required a shorter contact period, which proved the better cycling stability. This enhancement can be explained by structural stabilization and active site retention of carbonaceous nature, and the progressive degradation might be due to the partial blockage and incomplete desorption of the sites during the EDTA washing (Ebrahimzadeh and Akbari, 2025).

Table 4. Thermodynamic parameters (ΔH°, ΔS°, and ΔG° at 298 K) for methylene blue adsorption onto CS and CS/DPB

Adsorbent	ΔH° (kJ/mol)	ΔS° (J/mol·K)	ΔG° (kJ/mol) at 298 K
CS	-3.36	-136.9	-4.13
CS/DPB	-12.55	-10.44	-9.89

Table 5. Comparison of recent literature on methylene blue removal using low-cost/sustainable adsorbents with the present work

Adsorbent	pH	q_{max} (mg/g)	Best isotherm	Best kinetic	Reference
Magnetic chitosan/biochar	6.5	21.4	Langmuir	PSO	(Zeng et al., 2015)
CS/sawdust biochar composite	6	24.6	Langmuir	PSO	(Fayad et al., 2025)
Chitosan/activated carbon	7	22.5	Langmuir	PSO	(Ebrahimzadeh and Akbari, 2025)
Acid-modified grape leaves	7	28.8	Langmuir	PSO	(Al-Qaim et al., 2024)
This work – CS	7	17.4	Langmuir	PSO	This study
This work – CS/DPB	7	30.3	Langmuir	PSO	This study

Note: PSO – pseudo-second order, q_{max} – maximum adsorption capacity, CS/DPB – chitosan/date-pit biochar composite.

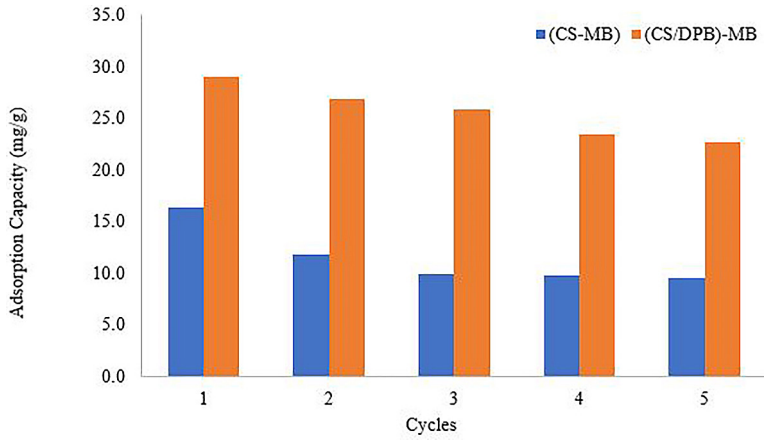

Figure 15. Regeneration of raw chitosan and date-pit charcoal–supported chitosan (CS/DPB) during the adsorption of methylene blue

ENVIRONMENTAL AND PRACTICAL FEASIBILITY OF THE COMPOSITE ADSORBENT

The conclusions stand on the significance of transforming date pits to carbonaceous sorbents to treat water as part of a sustainability-oriented process, particularly when paired with biopolymers to form high-performance adsorbents. The CS/DPB composite combines both the active functional groups of chitosan (NH_2/OH) and the great surface area and porosity of biochar, and improves the rapid and efficient binding of methylene blue under a realistic working environment (Abdulhameed et al., 2025). Also, such products as biochar/activated carbon created with date-palm waste help in the context of the circular economy and provide a cost-effective and scalable solution in dye-contaminated effluents treatment, even during changes in the quality of the influent (Kainth et al., 2024).

The CS/DPB composite has superior stability and better MB removal using the operating conditions compared to using raw chitosan, and this is owing to the synergy of chitosan functional groups and the porous carbonaceous structure of date-pit biochar, which offers multiple binding sites and mechanisms. The kinetic and equilibrium modeling suggested that it was mainly a monolayer (Langmuir) adsorption and a pseudo-second order behavior. Besides, the temperature effect is not only indicative of the thermodynamic considerations but also of the kinetic constraints and structural characteristics of the adsorbents.

The CS/DPB composite has a great economic advantage that is upheld by the concepts of the circular economy since the used date pits as a low/free cost agricultural waste will be locally found, and the need to rely on commercial active carbon at a high cost will be eliminated. Replacement of 40% chitosan with 40% biochar decreases the quantity of chitosan (the most expensive ingredient) and improves adsorption capacity by approximately one-fourth of raw chitosan but does not cause any loss in performance during repeated cycles. That is why it is an economical and viable solution to the dye-contaminated wastewater treatment, in particular, the treatment of textile or leather effluents in the adsorption columns or fixed-bed filters. Its high removal over a broad pH region and simple recyclability minimize the operation costs by necessitating no pH adjustment and the switching of adsorbents, resulting in the sustainability of treatment and the circular-economy model in operation.

The future studies can be based on the measurement of the performance of CS/DPB composite under real wastewater with a mixture of competing contaminants to estimate its selectivity and strength in real conditions. Besides that, continuous flow column studies are suggested to help in scale-up and practical implementation. More optimization of the composite formulation and biochar preparation state should lead to an improvement in mechanical stability and long-term performance. Lastly, techno-economic analysis and life-cycle analysis must be carried out to have a comprehensive assessment of the environmental and economic viability of this sustainable adsorption system.

CONCLUSIONS

A chitosan/date-pit biochar composite and raw chitosan were analyzed based on the removal of the MB in the batch system. CS/DPB had greater and more consistent removal and took a shorter time to achieve equilibrium than CS. The analysis at the isotherm revealed that the Langmuir model was better suited to the MB adsorption on both adsorbents (monolayer adsorption predominant), with Freundlich giving a relatively poor description, particularly when it comes to the composite. The pseudo-second order model was the best way to represent kinetic data. The thermodynamic findings supported the idea that the adsorption of MB is spontaneous, whereby CS/DPB has a greater force of action. In general, CS/DPB is an economic and environmentally suitable sorbent in the treatment of MB-contaminated water.

REFERENCES

1. Abbas, S., Javeed, T., Zafar, S., Taj, M. B., Ashraf, A. R., Din, M. I. (2021). Adsorption of crystal violet dye by using a low-cost adsorbent–peanut husk. *Desalination and Water Treatment*, *233*, 387–398.
2. Abd El-Monaem, E. M., Omer, A. M., El-Subruiti, G. M., Mohy-Eldin, M. S., Eltaweil, A. S. (2024). Zero-valent iron-supported lemon-derived biochar for ultra-fast adsorption of methylene blue. *Biomass Conversion and Biorefinery*, *14*(2), 1697–1709.
3. Abdulhameed, A. S., Al Omari, R. H., Althahban, S., Jazaa, Y., Abualhaija, M., Algburi, S. (2025). Green vegetable waste composited with chitosan as a bioadsorbent for effective removal of methylene blue dye from water: Insight into physicochemical and adsorption characteristics. *Biomass and Bioenergy*, *193*, 107528.
4. Ahmed, S. H., Abduljabbar, R. A. (2023). Removal of methylene blue dye from aqueous solutions using cordia myxa fruits as a low-cost adsorbent. *Tikrit Journal of Engineering Sciences*, *30*(3), 90–99.
5. Ahmed, S. H., Rasheed, E. A., Rasheed, L. A., Abdulrahim, F. R. (2024). Decolorization of cationic dye from aqueous solution by Multiwalled Carbon Nanotubes. *Journal of Ecological Engineering*, *25*(2).
6. Al-Ghouti, M. A., Da'ana, D. A. (2020). Guidelines for the use and interpretation of adsorption isotherm models: A review. *Journal of Hazardous Materials*, *393*, 122383.
7. Alhemadan, A. H., Akhtar, K., Bakhsh, E. M., Homdi, T. A., Khan, S. B. (2025). Design of switchable adsorbent based on chitosan and date palm endocarp film for adsorption of cationic and anionic dyes from aqueous solution. *International Journal of Biological Macromolecules*, *306*, 141362.
8. Aljeboree, A. M., Alshirifi, A. N., Alkaim, A. F. (2017). Kinetics and equilibrium study for the adsorption of textile dyes on coconut shell activated carbon. *Arabian Journal of Chemistry*, *10*, S3381–S3393.
9. Badran, I., Khalaf, R. (2020). Adsorptive removal of alizarin dye from wastewater using maghemite nanoadsorbents. *Separation Science and Technology*, *55*(14), 2433–2448.
10. Bambal, A., Gaydhane, A., Chute, A., Sarvanan, D., Jugade, R. (2025). Novel chitosan-magnetite-silica ternary capsules for highly efficient sequestration of reactive dyes from aqueous media. *Environmental Research*, *275*, 121359.
11. Chieng, H. I., Lim, L. B. L., Priyantha, N. (2017). Enhancement of crystal violet dye adsorption on Artocarpus camansi peel through sodium hydroxide treatment. *Desalination and Water Treatment*, *58*, 320–331.
12. Dastoom, Z. (2023). Production of Ni0. 5Co0. 5Fe_2O_4/activated carbon@ chitosan magnetic nanobiocomposite as a novel adsorbent of methylene blue in aqueous solutions. *Scientific Reports*, *13*(1), 6137.
13. Ebrahimzadeh, F., Akbari, A. (2025). Investigation the adsorption mechanisms, chemical resistance and mechanical strength of the synthesized chitosan/activated carbon composite in methylene blue removal. *Scientific Reports*, *15*(1), 37820.
14. Fegade, U., Kolate, S., Dhake, R., Inamuddin, Altalhi, T., Kanchi, S. (2021). Adsorption of Congo Red on Pb doped FexOy: experimental study and theoretical modeling via double-layer statistical physics models. *Water Science and Technology*, *83*(7), 1714–1727.
15. Gamal, D., Abd-Elkhalek, A., Shaban, M., Al-Saeedi, S. I., Elbasiony, A. M., El-Aziz, G. H. A., Mohamed, F. (2025). Insights into the Structure and Removal Performance of Cationic Dyes by Adsorption onto MgAl LDH-Chitosan/Serpentine Nanocomposite. *Journal of Inorganic and Organometallic Polymers and Materials*, 1–22.
16. Gao, N., Du, W., Zhang, M., Ling, G., Zhang, P. (2022). Chitosan-modified biochar: Preparation, modifications, mechanisms and applications. *International Journal of Biological Macromolecules*, *209*, 31–49.
17. Goksu, A., Tanaydin, M. K. (2017). Adsorption of hazardous crystal violet dye by almond shells and determination of optimum process conditions by the Taguchi method. *Desalination and Water Treatment*, *88*, 189–199.
18. Hevira, L., Ighalo, J. O., Sondari, D. (2024). Chitosan-based polysaccharides for effective synthetic dye adsorption. *Journal of Molecular Liquids*, *393*, 123604.
19. Hosney, A., Urbonavičius, M., Varnagiris, Š., Ignatjev, I., Ullah, S., Barčauskaitė, K. (2025).

Feasibility study on optimizing chitosan extraction and characterization from shrimp biowaste via acidic demineralization. *Biomass Conversion and Biorefinery*, *15*(8), 12673–12687.

20. Huang, L., Wang, M., Shi, C., Huang, J., Zhang, B. (2014). Adsorption of tetracycline and ciprofloxacin on activated carbon prepared from lignin with H_3PO_4 activation. *Desalination and Water Treatment*, *52*(13–15), 2678–2687.
21. Ibrahim, A. K., Ahmed, S. H., Abduljabbar, R. A. (2024). Adsorption of Congo Red dye from aqueous solutions using an eco-friendly adsorbent derived from buckthorn fruits. *Tikrit Journal of Engineering Sciences*, *31*(1), 182–192.
22. Ibrahim, A., Yaser, A. Z., Lamaming, J. (2021). Synthesising tannin-based coagulants for water and wastewater application: A review. *Journal of Environmental Chemical Engineering*, *9*(1), 105007.
23. Kainth, S., Sharma, P., Pandey, O. P. (2024). Green sorbents from agricultural wastes: A review of sustainable adsorption materials. *Applied Surface Science Advances*, *19*, 100562.
24. Kellner-Rogers, J. S., Taylor, J. K., Masud, A. M., Aich, N., Pinto, A. H. (2019). Kinetic and thermodynamic study of methylene blue adsorption onto chitosan: Insights about metachromasy occurrence on wastewater remediation. *Energy, Ecology and Environment*, *4*(3), 85–102.
25. Loryuenyong, V., Nakhlo, W., Srikaenkaew, P., Yaidee, P., Buasri, A., Eiad-Ua, A. (2024). Enhanced CO_2 capture potential of chitosan-based composite beads by adding activated carbon from coffee grounds and crosslinking with epichlorohydrin. *International Journal of Molecular Sciences*, *25*(16), 8916.
26. Ma, L., Su, C., Li, X., Wang, H., Luo, M., Chen, Z., Zhang, B., Zhu, J., Yuan, Y. (2024). Preparation and characterization of bilayered microencapsulation for co-delivery *Lactobacillus casei* and polyphenols via Zein-chitosan complex coacervation. *Food Hydrocolloids*, *148*, 109410.
27. Mahdi, Z., El Hanandeh, A., Yu, J. (2015). Date palm (*Phoenix Dactylifera* L.) seed characterization for biochar preparation. *EPPM 2015*.
28. Manubolu, M., Pathakoti, K., Leszczynski, J. (2024). Recent advances in chitosan-based nanocomposites for dye removal: a review. *International Journal of Environmental Science and Technology*, *21*(4), 4685–4704.
29. Neusatz Guilhen, S., Watanabe, T., Tieko Silva, T., Rovani, S., Takehiro Marumo, J., Alberto Soares Tenório, J., Mašek, O., Goulart de Araujo, L. (2022). Role of point of zero charge in the adsorption of cationic textile dye on standard biochars from aqueous solutions: selection criteria and performance assessment. *Recent Progress in Materials*, *4*(2), 1–30.
30. Nodehi, R., Shayesteh, H., Kelishami, A. R. (2020). Enhanced adsorption of Congo Red using cationic surfactant functionalized zeolite particles. *Microchemical Journal*, *153*, 104281.
31. Nuruzzaman, M., Mondal, M. I. H. (2025). Nano-Chitosan-coated sand: A sustainable superadsorbent for removal of heavy metals and dye particles from industrial effluents. *Environmental Nanotechnology, Monitoring & Management*, 101076.
32. Okorocha, N. J., Omaliko, C. E., Osuagwu, C. C., Chijioke-Okere, M. O., Enenebeaku, C. K. (2021). Utilization of agro-waste in the elimination of dyes from aqueous solution: Equilibrium, kinetic, and thermodynamic studies. *International Letters of Chemistry, Physics and Astronomy*, *86*, 11–23.
33. Osterrieth, J. W. M., Rampersad, J., Madden, D., Rampal, N., Skoric, L., Connolly, B., Allendorf, M. D., Stavila, V., Snider, J. L., Ameloot, R. (2022). How reproducible are surface areas calculated from the BET equation? *Advanced Materials*, *34*(27), 2270205.
34. Parlayıcı, Ş., Baran, Y. (2025). A novel alginate/fruit waste/Fe_3O_4 hydrogel biobeads for highly efficient removal of methylene blue from aqueous solution. *Polymer Bulletin*, 1–49.
35. Patel, P. K., Uppaluri, R. V. S. (2025). Environmental sustainability through adsorption: A review of chitosan's potential in dye pollution remediation. *Sustainable Chemistry and Pharmacy*, *46*, 102096.
36. Peramune, D., Manatunga, D. C., Dassanayake, R. S., Premalal, V., Liyanage, R. N., Gunathilake, C., Abidi, N. (2022). Recent advances in biopolymer-based advanced oxidation processes for dye removal applications: A review. *Environmental Research*, *215*, 114242.
37. Rápó, E., Tonk, S. (2021). Factors affecting synthetic dye adsorption; desorption studies: A review of results from the last five years (2017–2021). *Molecules*, *26* (17), 5419.
38. Rasheed, E., Humadi, J. I., Ahmed, S. H., Rasheed, L. A. A. (2026). Orange peel-derived bio-adsorbents for methylene blue removal: Surface characteristics, experiments, kinetics, and density functional theory mechanism. *South African Journal of Chemical Engineering*, 100850.
39. Roy, H., Prantika, T. R., Riyad, M. H., Paul, S., Islam, M. S. (2022). Synthesis, characterizations, and RSM analysis of Citrus macroptera peel-derived biochar for textile dye treatment. *South African Journal of Chemical Engineering*, *41*, 129–139.
40. Sharma, P., Sharma, S., Sharma, S. K., Yifei, S., Guo, F., Ichikawa, T., Jain, A., Shrivastava, K. (2024). Evaluation of optimized conditions for the adsorption of malachite green by SnO_2-modified sugarcane bagasse biochar nanocomposites. *RSC Advances*, *14* (40), 29201–29214.
41. Shehab, M. A., Al-Lami, M., Taher, M. A., Mohammed, H. H., AbdulRazak, A. A., Rashid, K. T.,

Mahmood, A., Abd Al-Ogaili, M. F., Alsarayefi, S. (2025). Recent progress in adsorptive

42. Song, L., Liu, M., Nian, M., Yang, G. (2024). Preparation of HMn_2O_4 lithium-ion sieves with low manganese dissolution loss for improved cycling stability. *RSC Advances*, *14*(28), 19795–19805.
43. Sulyman, M., Sienkiewicz, M., Haponiuk, J., Zalewski, S. (2018). New approach for adsorptive removal of oil in wastewater using textile fibers as an alternative adsorbent. *Acta Scientific Agriculture*, *2*(6), 1–6.
44. Sun, R., Lv, R., Li, Y., Du, T., Chen, L., Zhang, Y., Zhang, X., Zhang, L., Ma, H., Sun, H. (2023). Simple and sensitive electrochemical detection of sunset yellow and Sudan I in food based on AuNPs/Zr-MOF-Graphene. *Food Control*, *145*, 109491.
45. Vigneshwari, S., Gokula, V. (2018). Extraction and FTIR characterization of chitosan from *Portunus pelagicus* (Linnaeus, 1758) shell wastes. *International Journal of Advanced Scientific Research and Management, 3*(10).
46. Yao, X., Ji, L., Guo, J., Ge, S., Lu, W., Cai, L., Wang, Y., Song, W., Zhang, H. (2020). Magnetic activated biochar nanocomposites derived from wakame and their application in methylene blue adsorption. *Bioresource Technology*, *302*, 122842.
47. Zhou, P., Li, X., Zhou, J., Peng, Z., Shen, L., Li, W. (2023). Insights into the adsorption mechanism of methylene blue on biochar from phytoextraction residues of *Citrus aurantium* L.: Adsorption model and DFT calculations. *Journal of Environmental Chemical Engineering*, *11*(5), 110496.